Digital Simulation of Voltage Regulated Inverter for FLC Controlled Autonomous PV-Wind Hybrid Power System

A. V. Pavan Kumar[1] **Alivelu M. Parimi[2]**
[1, 2] Department of EEE, BITS-Pilani, Hyderabad Campus, Jawahar Nagar,
Shamirpet, Hyderabad, T.S, India. (pawanrao82@gmail.com[1], alivelu@hyderabad.bits-pilani.ac.in[2])

K. Uma Rao[3]
[3]Department of EEE, R. V College of Engineering, Mysore Road,
Bengaluru, Karnataka, India. (drumarao@yahoo.co.in[3])

Abstract: *The solar PV and the wind are comprehensively measured to be a spotless form of energy harvest from Renewable Energy Sources (RES) which can calm grid reliance. The PV and wind power advances being entrenched, infiltration of these RES into the system has increased exponentially. All together to outline appropriate control and tackle power through RES, the information regarding environmental conditions of the location is crucial. A hybrid power system consisting of solar PV and wind power are chosen for the study. The output from wind power is changed to DC supply and consolidated with PV to make the framework recurrence and autonomous of environmental changes. The effectiveness to maintain DC voltage consistent at desired level is accomplished by Fuzzy Logic Control (FLC) controlled boost converter and the Maximum Power Point Tracker (MPPT) to concentrate on the maximum power. The Voltage Regulated Inverter (VRI) is used to invert DC to AC, a control based on discrete PLL is actualized in hybrid framework to maintain the parameters at desired level. A mathematical model of hybrid framework consisting of FLC-based MPPT controller boost converters and VRI for standalone application is executed in MATLAB, Simulink. The execution of VRI under steady and differing AC load is dissected. Simulation results demonstrates satisfactory operation of inverter control logic.*

Key words: *VRI, solar illumination, Wind speed, FLC, Stand-alone system, Inverter control, Load frequency control.*

1. Introduction.

A Hybrid Power system is a combination of different forms of RES like Fuel Cell, Wind, and Photovoltaic (PV) etc. are integrated for better clean source of energy generation. In order to select RES for the autonomous operation, the knowledge of environmental conditions is essential. The key downside of the autonomous hybrid system is to have a stable operating frequency and supply voltage is 415 V at 50Hz frequency in India [1]. Different topologies of power electronics converters were proposed in the literature by various researchers Arafat, M.N et. al [2] has worked towards seamless transitions between grid connected and islanded mode of operation of utility inverter. A space vector PWM technique is employed to generate grid angle in order to control the inverter output voltage. Ariany, M. et. Al [3] has proposed a Phase Locked Loop (PLL) based inverter voltage control of islanded microgrid. A voltage, current and frequency control logic were implemented to have a stable operation of the islanded microgrid. Ozdemir, E. et. al [4] has assessed the enactment of a 7.2 kW PV generation for rural electrification. Rong- Jong Wai et. al [5] a comparative analysis of simulation model with the real-time system was done and by the analysis it has been concluded that the simulated model results have viable results and different topologies of inverters for autonomous mode of operation were suggested in the literature [6]–[9].

Large amount of work was done toward improvement of the Maximum Power Point Tracker (MPPT) algorithm of RES generation and ideal location of placement and different renewable energy in the power network, energy management system of grid connected RES generation, and optimization. In stand-alone mode computation of reference phase angle θ and to sustain output frequency and Voltage constant requires different loops of control implementation. In order to have an enhanced control, a discrete PLL is employed instead of conventional PLL to control the inverter. The input to the discrete PLL are the desired frequency and phase angle depending on the desired values of the θ is computed. Which makes the design of control logic simpler for implementation. In the literature inverter based control of micro grids a DC source is considered in the studies instead of RES generation. The dynamics of fluctuations produced due to RES generations are not considered which plays a vital role in the design of inverter control.

No work was reported towards the performance analysis of hybrid power system with Discrete PLL. The proposed inverter control logic implementation using discrete PLL to estimate the phase angle θ to enhance the inverter control. Instead of having a complicated inverter control with several stages of

voltage, current and frequency control. With the above backdrop, a simulation study of the standalone hybrid power system with AC load under different loading conditions. The following section will discuss the equation based analysis of the hybrid power system.

2. Modeling of Hybrid Power System:

Figure 1 shows the graphical representation of PV-Wind hybrid power system which consists of Solar PV based, Wind based generation, and Voltage regulated inverter feeding AC load.

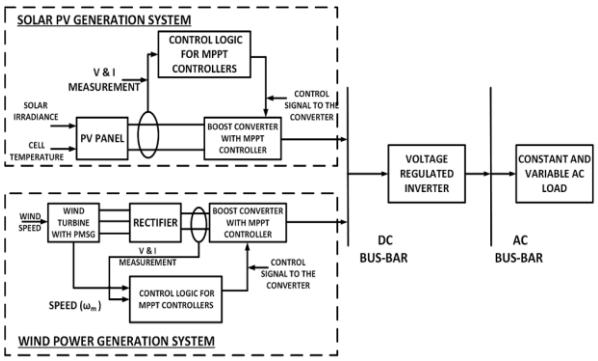

Fig. 1 Graphical representation of hybrid system

2.1 Solar Photovoltaic generation:

The building blocks of Solar Photovoltaic generation are PV cell, Boost converter and the duty cycle is controlled by Perturb and Observe (P & O) MPP (maximum power point) tracking algorithm. The electrical equivalent of PV cell is shown in Fig. 2.

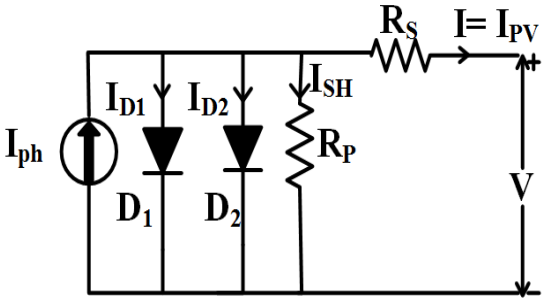

Fig. 2 Electrical equivalent of two diode model of PV cell

The electrical equivalent of PV cell with components current source I_{ph}, output voltage V , diodes D_1, D_2 with currents in diode I_{D1}, I_{D2}, Contact Resistor R_s, Internal Resistance R_p, current through shunt resistance I_{SH} and the output current I or I_{PV}. The output current of the PV cell (1).

$$I_{pv} = I_{PH} - I_{D1} - I_{D2} - I_{SH} \quad (1)$$

where, I_{D1}, I_{D2} are the diode diffusion currents rewriting (1) into (2).

$$I = I_{ph} - I_s\left[e\left(\frac{V + R_s \times I}{N \times V_t}\right) - 1\right] - I_{s2}\left[e\left(\frac{V + R_s \times I}{N_2 \times V_t}\right) - 1\right] - \frac{V + R_s \times I}{R_p} \quad (2)$$

where I_{s1}, I_{s2} are the reverse saturation currents, N_1,N_2 are the quality factors of diode D_1,D_2, thermal voltage V_t is defined by (3) with series connected cells being N_s, k is the Boltzmann constant, q charge on an electron, T-junction temperature.

$$V_t = \frac{N_s \times k \times T}{q} \quad (3)$$

A Simulink model of PV panel is developed with the help of the equation based modelling of the PV cell [10]. The electrical parameters of simulated PV panel are extracted from data-sheet of SHARP NUU245P1 are shown in Table. 1 is at standard test conditions. A 15 kW PV generation is achieved by connecting 10 PV panels in series forming a string thus generating a voltage of 304 V at Maximum Power Point (MPP) and such 7 strings are connected in parallel to acquire a current of 56.56 A at MPP and the simulated P-V characteristics of PV generation at operating temperature of 250C and varying solar illumination levels is shown in Fig. 3.

Table 1
Electrical Parameters of PV panel and PV generation

Electrical Parameters at 1000 W / m^2 at 25^0C			
	Data Sheet	PV Panel	PV Generation
Open Circuit Voltage (V_{oc})	37.3 V	37.3 V	373 V
Short Circuit Current (I_{sc})	8.7 A	8.709 A	60.9 A
Voltage at P_{max}	30.4 V	30.75 V	304 V
Current at P_{max}	8.08 A	7.97 A	56.56 A
Maximum Power (P_{max})	245 W	245.06 W	17, 197 W

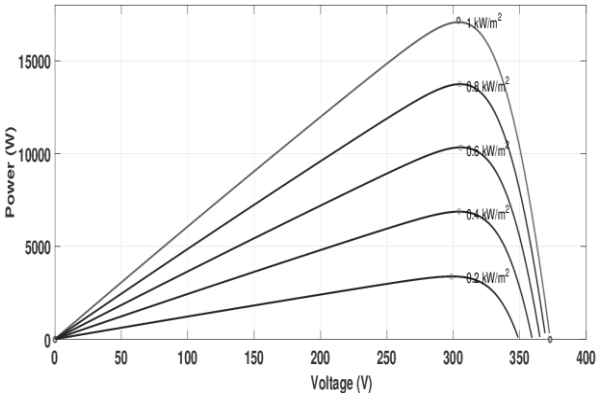

Fig. 3 Simulated P-V Characteristics of PV generation under different solar illumination levels

2.2 PMSG based wind Power generation:
The basic building blocks of wind generation as shown in block diagram of hybrid system Fig. 1 are Wind turbine which converts captured wind energy into mechanical energy, Permanent Magnet Synchronous Generator (PMSG) to convert mechanical energy into electrical, Diode rectifier, and Hill climb search (HCS) MPPT algorithm. The mechanical power Po which is expressed as (4).

$$P_o = \frac{1}{2}\rho A V^3 C_p \quad (4)$$

where,
P_o = Output power from wind turbine (W),
ρ = air density (Kg/m^3),
A = area swept by the rotor blades (m^2),
V = velocity of the air (m/s), and
C_p= Co-efficient of power.

The Co-efficient of power C_p from (4) The C_p is expressed in terms of tip-speed ratio λ and blade pitch angle θ as (5).

$$C_p(\lambda,\theta) = C_1\left(C_2\frac{1}{\beta} - C_3\beta\theta - C_4\theta^x - C_5\right)e^{-C_6\frac{1}{\beta}} \quad (5)$$

The values of coefficients C_1=0.5176, C_2=116, C_3=0.4, C_4= 5, C_5=21, C_6=0.0068 and value of x can be determined by turbine utilized and β is defined as:

$$\frac{1}{\beta} = \frac{1}{\lambda + 0.08\theta} - \frac{0.035}{1+\theta^3} \quad (6)$$

The mechanical torque T_m is expressed as (7).

$$T_m = \frac{P_m}{\omega_m} \quad (7)$$

where ω_m = Rotor angular speed (rad/s)

$$\omega_m = \frac{\lambda V}{R} \quad (8)$$

where, R defines wind turbine rotor radius in meters. A Simulink implementation of wind turbine based on the equation based modelling discussed [11].

The electrical torque of the PMSG is expressed as (9).

$$T_e = \frac{3}{2}\left(\frac{p}{2}\right)\left(\lambda o i_q + (L_d - L_q) i_q i_d\right) \quad (9)$$

where,
L_d, L_q = direct and quadrature-axis Inductance of (H)
λ_o = the amount of flux by permanent magnets (wb),
i_d, i_q = d and q- axis current in (A),
p = a number of pole pairs.

As $L_q = L_d$ the torque equation is rewritten as:

$$T_e = 1.5 p i_q \lambda_o \quad (10)$$

The load torque is expressed as (11).

$$T_m = T_e + D\omega_m + J\frac{d\omega_m}{dt} \quad (11)$$

Power output of PMSG is proportional to the velocity of the wind. As the velocity of wind varies generated voltage and its frequency varies. To make the output constant at desired level the voltage rectified using a full bridge diode rectifier as shown in Fig. 4.

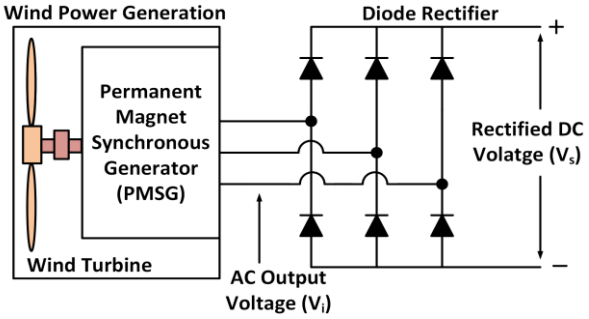

Fig. 4 Rectified output from Wind generation

The DC output from both RES generations are enhanced to anticipated level of 600 V using FLC-based boost converter and combined to form a common DC bus-bar as shown in Fig.1.

2.3 FLC-based MPPT controlled boost converter:

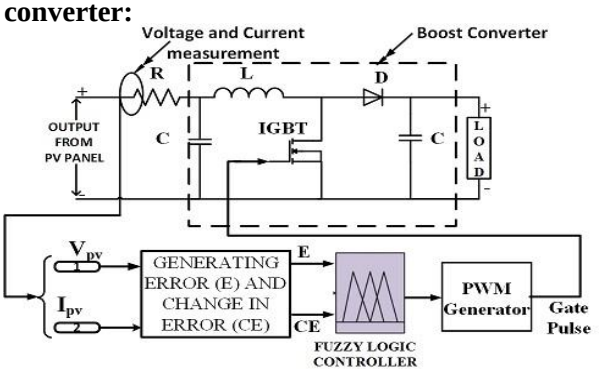

Fig. 5 Block diagram of boost converter for PV generation

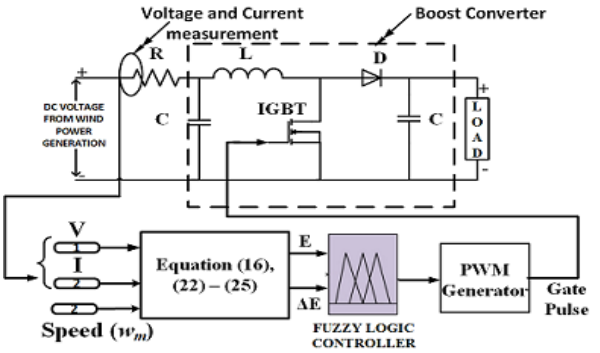

Fig. 6 Block diagram of boost converter for Wind generation

The block diagram of FLC based boost converters are graphically resented in Fig. 5 and Fig. 6 for PV and wind generation respectively. The output voltage o boost converter is computed as [12].

$$V_s DT = (V_o - V_s)(1-D)T \tag{12}$$

where D is the duty cycle of the converter and T is the time period. The boosted dc voltage can be expressed as (13)

$$\frac{V_o}{V_s} = \frac{1}{1-D} \tag{13}$$

a) MPPT algorithm under consideration:

The P&O algorithm is utilized to track the maximum power point (MPP) of the PV generation system and the flow chart of P & O algorithm is as shown in Fig. 7.

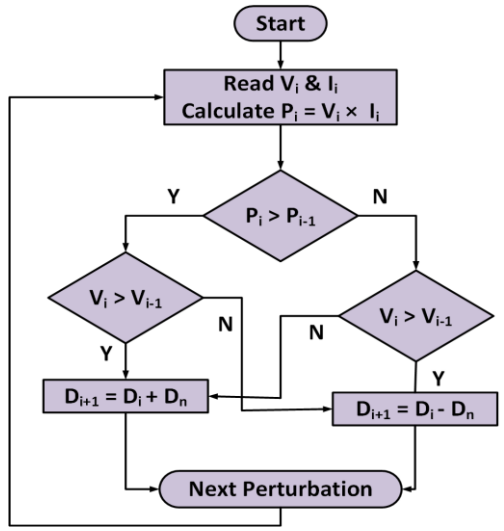

Fig. 7 Flow chart of P&O algorithm

HCS algorithm is employed to track the MPP of the wind-based generation system as shown in Fig. 8 and the MPP tracking process is realistically represented.

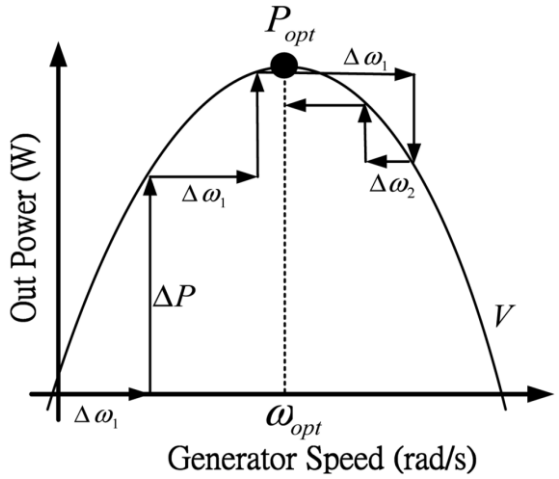

Fig. 8 Graphical representation of MPP

b) Fuzzy implementation of P & O algorithm:

The voltage (V_{pv}), current (I_{pv}) are sensed from the output of PV generation which are utilized to compute the control input to the fuzzy controller as shown in Fig. 5. The error (E) and change in error (CE) are computed (14)-(19) which are implemented in the subsystem shown in Fig. 5 [13].

$$P = V \times I \tag{14}$$

$$\Delta V = V(k) - V(k-1) \tag{15}$$

$$\Delta I = I(k) - I(k-1) \tag{16}$$

$$\Delta P = P(k) - P(k-1) \tag{17}$$

$$E = \frac{\Delta P}{\Delta V} \tag{18}$$

$$CE = E(k) - E(k-1) \tag{19}$$

where (k) is the current state of measured value and (k−1) is the previous state of measured value. The rule base of fuzzy logic implementation of P & O algorithm is shown in Table. 2 where NB_{pv} = Negativebig, NM_{pv}=Negativemedium, NS_{pv} = Negativesmall, ZE_{pv} = Zero, PS_{pv} =Positivesmall, PM_{pv}=Positivemedium, PB_{pv} = Positivebig.

Table 2
Fuzzy rule base for P & O algorithm

E	CE						
	NB_{pv}	NM_{pv}	NS_{pv}	ZE_{pv}	PS_{pv}	PM_{pv}	PB_{pv}
NB_{pv}	ZE_{pv}	ZE_{pv}	ZE_{pv}	NB_{pv}	NB_{pv}	NB_{pv}	NB_{pv}
NM_{pv}	ZE_{pv}	ZE_{pv}	ZE_{pv}	NM_{pv}	NM_{pv}	NM_{pv}	NM_{pv}
NS_{pv}	NS_{pv}	ZE_{pv}	ZE_{pv}	NS_{pv}	NS_{pv}	NS_{pv}	NS_{pv}
ZE_{pv}	NM_{pv}	NS_{pv}	ZE_{pv}	ZE_{pv}	ZE_{pv}	PS_{pv}	PM_{pv}
PS_{pv}	PM_{pv}	PS_{pv}	PS_{pv}	PS_{pv}	ZE_{pv}	ZE_{pv}	ZE_{pv}
PM_{pv}	PM_{pv}	PM_{pv}	PM_{pv}	ZE_{pv}	ZE_{pv}	ZE_{pv}	ZE_{pv}
PB_{pv}	PB_{pv}	PB_{pv}	PB_{pv}	ZE_{pv}	ZE_{pv}	ZE_{pv}	ZE_{pv}

c) Fuzzy Implementation of HCS algorithm:

As shown in Fig. 6 the voltage (V), current (I) are sensed at the input of boost converter and speed (ω_m) of the PMSG is sensed and given as input to compute the control input to the fuzzy implementation of the HCS algorithm. The error (E) and change in error (ΔE) are computed (14), (20)-(23) which are implemented in the subsystem shown in Fig. 6.

$$\Delta P = P(k) - P(k-1) \tag{20}$$

$$\Delta\omega_m = \omega_m(k) - \omega_m(k-1) \tag{21}$$

$$E = \frac{\Delta P}{\Delta\omega_m} \tag{22}$$

$$\Delta E = E(k) - E(k-1) \tag{23}$$

where (k) is the current state of measured value and ($k-1$) is the previous state of measured value. The conditions to track the MPP are

$$\frac{\Delta P}{\Delta \omega_m} = 0, \qquad (\omega_m = \omega_{mpp}) \tag{24}$$

$$\frac{\Delta P}{\Delta \omega_m} > 0, \qquad (\omega_m < \omega_{mpp}) \tag{25}$$

$$\frac{\Delta P}{\Delta \omega_m} < 0, \qquad (\omega_m > \omega_{mpp}) \tag{26}$$

The rule base of fuzzy logic implementation based on MPP tracking conditions given by (24)-(26) is shown in Table. 3 the suffix w is for wind power generation [13].

Table 3
Fuzzy rule base for HCS algorithm

E	ΔE				
	NB_w	NS_w	ZE_w	PS_w	PB_w
NB_w	ZE_w	ZE_w	NB_w	NB_w	NB_w
NS_w	NS_w	ZE_w	NS_w	NS_w	NS_w
ZE_w	NS_w	ZE_w	ZE_w	ZE_w	PB_w
PS_w	PS_w	PS_w	PS_w	ZE_w	ZE_w
PB_w	PB_w	PB_w	ZE_w	ZE_w	ZE_w

The fuzzy implementation of MPPT algorithm is realized in MATLAB, Simulink. The DC output voltage from PV and wind-based generation are stepped to the anticipated level and are kept stable at the desired level regardless of variation in environmental or load conditions.

3. Voltage Regulated Inverter (VRI) Control Design:

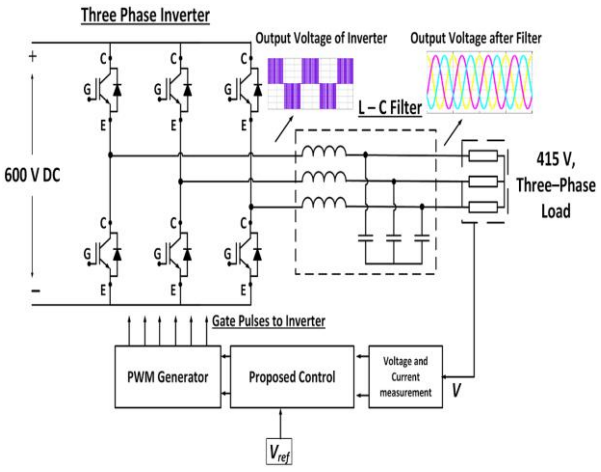

Fig. 9 Voltage Regulated Inverter control scheme

The element wise representation of the control scheme for the inverter is shown in Fig. 9. In the autonomous mode of operation VRI performs crucial role in hybrid power to keep the output parameters constant at anticipated level. The significant feature of VRI control compute the control signals to minimizing the error between measured and the reference value. The PWM triggering pulses are generated to control the output of the hybrid power system. This is achieved using the Synchronous Reference Frame (SRF) implementation of sensed signals and a discrete PLL to control and generate triggering signals.

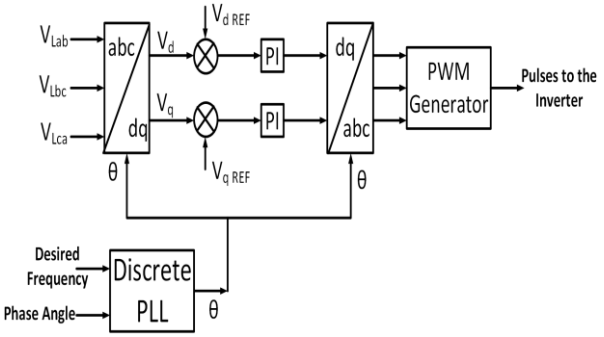

Fig. 10 Block diagram of proposed inverter control

The control logic schematics is graphically represented in Fig. 10. The output voltage V_{Labc} is sensed and is converted into $V_{\alpha\beta}$ and this $V_{\alpha\beta}$ reference frame using Clark transformation is expressed as (27) and (28) [14].

$$\begin{bmatrix} V_\alpha \\ V_\beta \end{bmatrix} = \frac{2}{3}\begin{bmatrix} 1 & -\frac{1}{2} & -\frac{1}{2} \\ 0 & -\frac{\sqrt{3}}{2} & \frac{\sqrt{3}}{2} \end{bmatrix}\begin{bmatrix} V_a \\ V_b \\ V_c \end{bmatrix} \tag{27}$$

$$\begin{bmatrix} V_d \\ V_q \end{bmatrix} = \begin{bmatrix} \cos\theta & -\sin\theta \\ \sin\theta & \cos\theta \end{bmatrix}\begin{bmatrix} V_\alpha \\ V_\beta \end{bmatrix} \tag{28}$$

A discrete PLL is used to generate the phase angel θ by computing with the desired frequency i.e. 50 Hz and angle 0^0. Control logic computes the control signal for the inverter depending on the phase estimated. The V_d, V_q computed are compared with the reference V_d = 1, V_q = 0 and PI controller is employed to minimize the error. The signal from PI controller is converted into abc reference frame and gating signals are created to regulate the switching action of the VRI.

4. The Concurrent data of Solar Illumination and Wind Speed:

The concurrent information of wind speed and solar illumination are recorded using a Climate Recording System (CRS) installed at Bits-Pilani, Hyderabad campus. The solar illumination and wind speed measured by the CRS are tabulated using a data logger. The average and maximum value of solar illumination and wind speed are measured and recorded in the said format. From the historical data considering one-day solar illumination and wind speed

data for investigating the performance of control logic implementation of VRI. The solar and wind speed data for a day are graphically represented in Fig. 11 and Fig. 12.

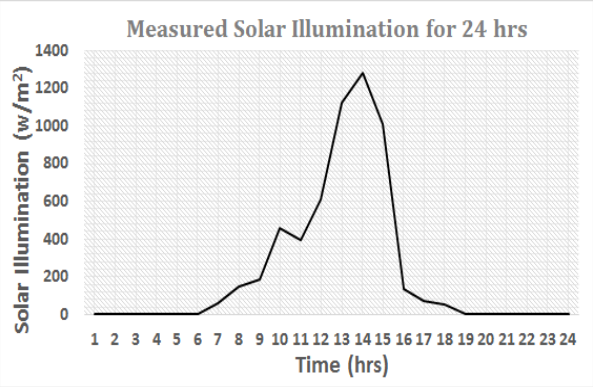

Fig. 11 24hr solar illumination profile measured

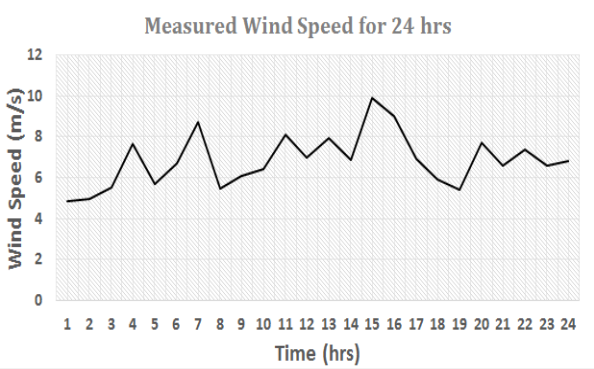

Fig. 12 24hr Wind speed profile measured

5. System Description and Simulation results:

A 20 kW MATLAB, Simulink model of a PV-Wind stand-alone system consisting of 5 kW Wind generation, 15 kW PV is implemented. The performance of control logic is analyzed under three distinct conditions (i) Persistent R-load of 20 kW, (ii) Varying load condition and the performance of VRI is investigated in terms of maintaining the parameters of the system constant.

5.1 Persistent R-load of 20 kW with instantaneous data of wind speed and solar illumination:

Performance of control logic implementation of VRI developed in Simulink is investigated with the recorded data of solar illumination, wind speed as shown Fig. 11, Fig. 12 under a persistent R-load of 20 kW. The desired control action is to maintain the parameters of the system constant under varying environmental conditions with a constant load on the system.

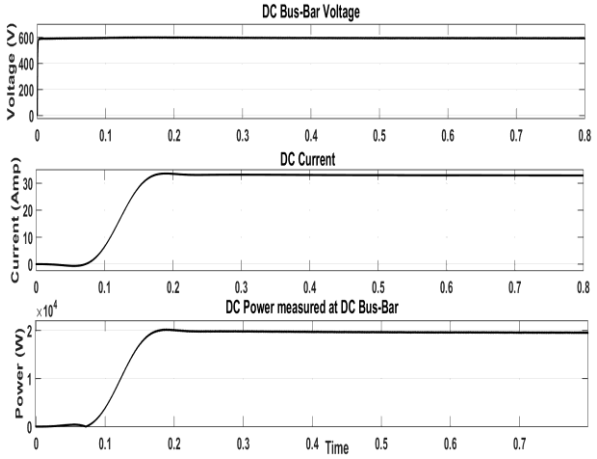

Fig. 13 Simulated DC Bus-Bar Voltage, Current, and Power

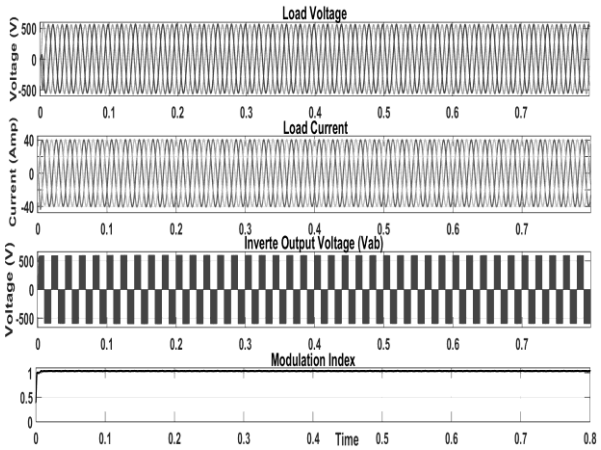

Fig. 14 Simulated AC load voltage, current, Inverter output voltage, and Modulation index

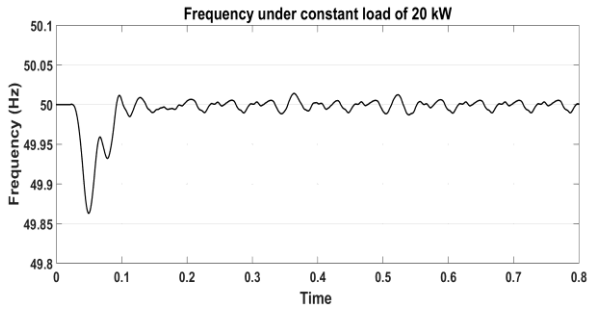

Fig. 15 Simulated frequency of Persistent R-Load

The simulated DC Bus-Bar Voltage, Current, and power inputted to the inverter are measured and graphically represented in Fig. 13. The system is simulated for 0.8 consider the scale of 0.1 is 1 hr as the PV based generation output is available from 8.00 am to 4.00 pm. It can be comprehended that the FLC-based MPPT controlled boost converter maintains the DC bus-bar voltage constant at 600 V and power transfer from both PV and Wind based generation irrespective of change in environmental condition.

Simulated AC Bus-Bar or load Voltage, current, inverter output Line voltage V_{ab} before filter and modulation index are plotted in Fig. 14. From the Fig. 14 it can be comprehended that the discrete based PLL control implementation maintained the AC bus-bar voltage constant. The graphically representation of simulated frequency is plotted in Fig. 15. It shows minor variation in frequency with maximum 0.2 % difference. The performance of inverter is computed and tabulated as shown in Table 4. The efficiency of the inverter at full load unity power factor under variable environmental conditions computed is 98.01%.

Table 4
The performance of the inverter under varying environmental and constant load condition.

	Voltage (V)	Current (A)	Power(W)
DC Bus-Bar	600	34.05	20,430
AC Bus-Bar	$V_{rms}=\frac{V_{peak}}{\sqrt{2}}=\frac{578}{\sqrt{2}}=409$	$\frac{40}{\sqrt{2}}=28.28$	$\sqrt{3}\times 409\times 28.25\times 1=20{,}033$
Efficiency of Inverter	$\frac{AC\,Power}{DC\ Power}$	$\frac{20{,}033}{20{,}430}\times 100$	98.01%

5.2 Variable resistive load with instantaneous information of wind speed and solar illumination:

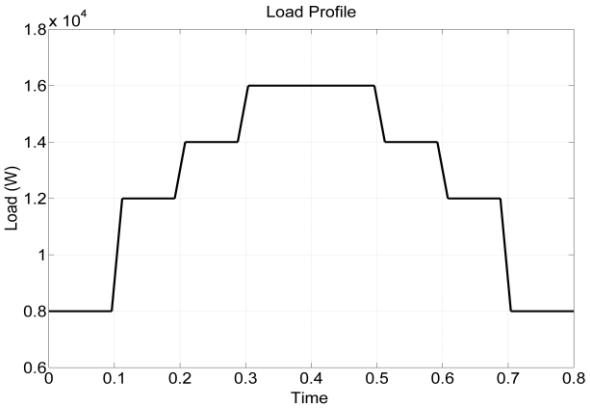

Fig. 16 varying resistive load pattern

The performance of control logic implementation of VRI developed is investigated with recorded data of solar illumination, wind speed as shown Fig. 11, Fig. 12 under variable resistive load as shown in Fig. 16. The desired control action is to maintain the output voltage and frequency of the PV-Wind hybrid system constant under varying environmental and load condition on the system. The simulated DC Bus- Bar Voltage, Current, and power inputted to the inverter are measured and graphically represented in Fig. 17. The system is simulated for 1.6 sec consider the scale of 0.1 is 30 min as the PV based generation output is available from 8.00 am to 4.00 pm and in order to have a clear understanding of the system under different loading condition. It can be comprehended that the FLC-based MPPT controlled boost converter maintains the DC bus-bar voltage constant at 600 V. Simulated AC Bus-Bar voltage, current, inverter output Line voltage V_{ab} before filter and modulation index are plotted in Fig. 18.

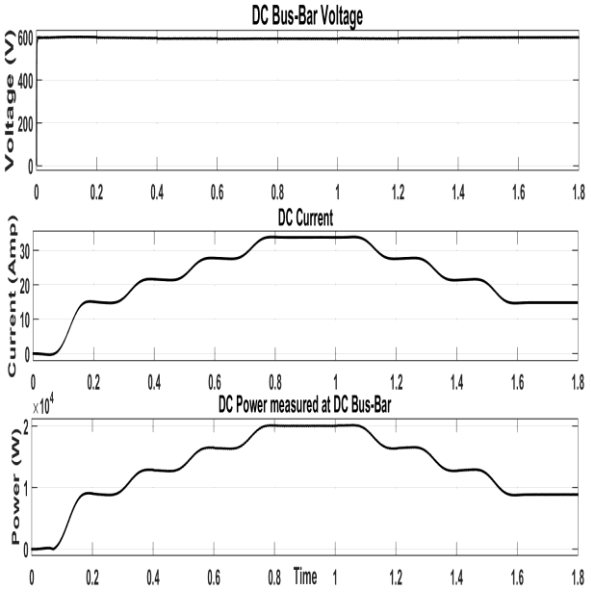

Fig. 17 Simulated DC Bus-Bar Voltage, Current, and Power

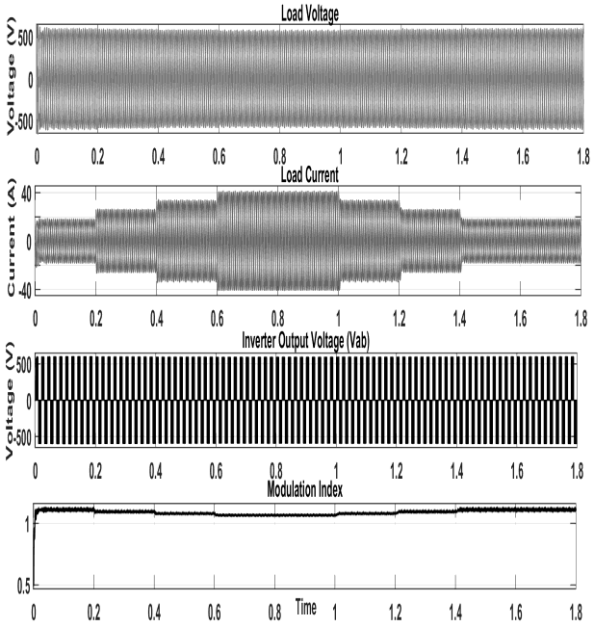

Fig. 18 Simulated Load Voltage, current, Inverter output voltage, and modulation index.

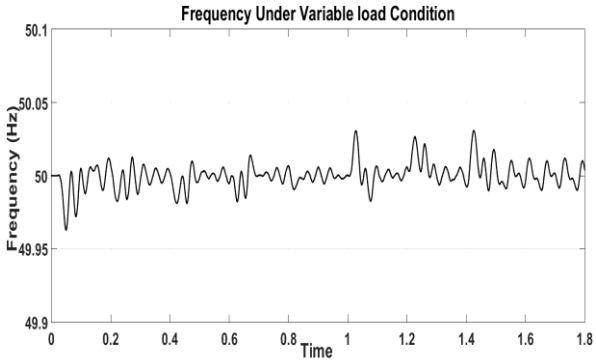

Fig. 19 Simulated system frequency

From Fig. 18 it can be apprehended that the discrete based PLL control implementation maintained the AC bus-bar voltage constant. Frequency of hybrid system is graphically represented in Fig. 19 it can be concluded that the control logic implementation of VRI worked as anticipated by maintaining the frequency at 50 Hz. The performance of inverter is computed and tabulated in Table 5.

Table 5
Performance of inverter

Time		Voltage (V)	Current (A)	Power (W)	Efficiency (%)
0-0.2	DC	600	14.66	8.800	98.7
1.6-1.8	AC	417	12.02	8,686	
0.2-0.4,	DC	600	21.33	12,800	95.8
1.2-1.4	AC	417	16.97	12,263	
0.4-0.6	DC	600	27.33	16,400	98.0
1.0-1.2	AC	410	22.63	16,073	
0.6-1.0	DC	600	34.05	20,430	98.01
	AC	409	28.28	20,033	

The frequency deviation of the system under two different loading conditions considered and simulated are tabulated as shown in Table 6. It is clear from the Table 6 that the maximum and minimum deviation of the system under two loading conditions simulated are 0.28 % and 0.02 %. The Discrete PLL based control logic implementation of inverter maintained the frequency of system within the limits of grid code [15].

Table 6
Frequency deviation of the system under two loading conditions considered

	Negative Freq. Deviation		Positive Freq. Deviation	
	Value	%	Value	%
Case (i)	49.86	0.28	50.01	0.02
Case (ii)	49.96	0.08	50.03	0.06

6. Conclusion:

In this paper implementation of VRI for 20 kW hybrid power system in MATLAB, Simulink is done. The Mathematical modeling of RES selected for the study i.e. Photovoltaic and Wind. FLC-based MPPT controlled boost converter is simulated. The performance of FLC-based boost converter and VRI are investigated for PV, Wind based generation individually and interconnected hybrid arrangement for varying load situations. In interconnected system, a common DC bus-bar with 600 V is formed and this DC voltage. The inverter controls the AC voltage with a magnitude of 415 V RMS and frequency 50 ± 1% Hz irrespective of change in load conditions. It can be concluded from the simulation results that the load voltage is sustained and frequency 50 Hz (50.03 Hz to 49.86 Hz) regardless of variation in load from 8 kW to 20 kW.

The proposed discrete PLL based control scheme operates as desired by maintaining the load frequency and voltage constant thereby increasing the reliability, efficiency of the system. Future work may include analyzing performance of the voltage regulated inverter for grid integration and realization of simulation results with a prototype model development.

Reference:

[1] Bhattacharjee, S , Acharya, S.: *PV–wind hybrid power option for a low wind topography.* In: Energy Convers. Manag., 89 (2015), pp. 942–954.

[2] Arafat, M.N, Elrayyah, A, Sozer, Y.: *An Effective Smooth Transition Control Strategy Using Droop-Based Synchronization for Parallel Inverters*. In: IEEE Trans. Ind. Appl., 51(2015), no. 3, May 2015, p. 2443–2454.

[3] Han, Y, Li, H, Shen, P, Coelho, E.A.A and Guerrero, J. M. : *Review of Active and Reactive Power Sharing Strategies in Hierarchical Controlled Microgrids*. In: IEEE Transactions on Power Electronics, 32(2017), no. 3, pp. 2427-2451.

[4] Ozdemir, E, Ozdemir, S, Tolbert, L. M. :

Fundamental-Frequency-Modulated Six-Level Diode-Clamped Multilevel Inverter for Three-Phase Stand-Alone Photovoltaic System. In: IEEE Trans. Ind. Electron., 56 (2009), No. 11, p. 4407–4415.

[5] Narejo, G. B, Azeem, F, and Ammar, M . Y: *A survey of control strategies for implementation of optimized and reliable operation of renewable energy based microgrids in islanded mode*. In *Power Generation System and Renewable Energy Technologies (PGSRET)*, Islamabad, 2015, pp. 1-5..

[6] Ochs, D. S, Mirafzal, B, Sotoodeh, P: *A Method of Seamless Transitions Between Grid-Tied and Stand-Alone Modes of Operation for Utility-Interactive Three-Phase Inverters.*In: IEEE Trans. Ind. Appl., 50 (2014), No. 3, p. 1934–1941.

[7] AlKaabi, S. S., Khadkikar, V and Zeineldin, H. H: Incorporating PV Inverter Control Schemes for Planning Active Distribution Networks. In: *IEEE Transactions on Sustainable Energy*, 6(2015), No. 4, pp. 1224-1233.

[8] Karimi, M-Ghartemani : *Universal Integrated Synchronization and Control for Single-Phase DC/AC Converters*. In: IEEE Trans. Power Electron., 30 (2015) , No. 3, p. 1544–1557.

[9] Egwebe, A. M, Fazeli, M, Igic, M and Holland, P. M.: *Implementation and Stability Study of Dynamic Droop in Islanded Microgrids*. In *IEEE Transactions on Energy Conversion*, 31(2016), No. 3, pp. 821-832.

[10] Pavan Kumar, A. V, Parimi, A. M, and Uma Rao, K.: *Performance Analysis of a Two-Diode model of PV cell for PV based generation in MATLAB*. In: IEEE International Conference on Advanced Communications, Control and Computing Technologies, 2014, p. 68–72.

[11] Kumar, A. V. P, Parimi, A. M, Rao, K. U.: *Investigation of small PMSG based wind turbine for variable wind speed*. In: International Conference on Recent Developments in Control, Automation and Power Engineering (RDCAPE), 2015, pp. 107–112.

[12] Rashid, M. H. : *Power Electronics Handbook.* Academic Press, 2001.

[13] Kumar, A. V. P, Parimi, A. M, Rao, K. U.: *Implementation of MPPT control using fuzzy logic in solar-wind hybrid power system*. In: IEEE International Conference on Signal Processing, Informatics, Communication and Energy Systems (SPICES), 2015, pp. 1–5.

[14] Surprenant, M, Hiskens, I, Venkataramanan, G: *Phase locked loop control of inverters in a microgrid*. In: IEEE Energy Convers. Congr. Expo.,2011, p. 667–672.

[15] Preda, T.N, Uhlen, K, Nordgård, D. E: *An overview of the present grid codes for integration of distributed generation*. In: CIRED Workshop: Integration of Renewables into the Distribution Grid, 2012, p. 20–20.

Nomenclature:

PV	-	Photovoltaic
PMSG	-	Permanent Magnet Synchronous Generator
RES	-	Renewable Energy Source
MPPT	-	Maximum Power Point Tracker
P & O	-	Perturb and Observe
HCS	-	Hill Climb Search
MPP	-	Maximum Power Point
FLC	-	Fuzzy Logic Control
PLL	-	Phase Lock Loop
VRI	-	Voltage Regulated Inverter
DC	-	Direct Current
AC	-	Alternate Current
PWM	-	Pulse Width Modulation
P-V	-	Power-Voltage
I-V	-	Current-Voltage
R-load	-	Resistive load
θ	-	Phase angle
E	-	Error
ΔE, CE	-	Change in Error
k	-	Current state
k-1	-	Previous state
ΔP	-	Change in Power
ΔV	-	Change in Voltage
ΔI	-	Change in current
V_{rms}	-	RMS value of the Voltage
V_{peak}	-	Peak value of the Voltage
V_{Labc}	-	Three phase line voltage
V_d, V_q	-	Direct and quadrature axis Voltage
CRS	-	Climate Recording System
SRF	-	Synchronous Reference Frame